A Three Phase Grid-Tied Solar Photovoltaic System with Improved Power Profile Using Modular Probabilistic Neural Network

Mohanram Gnanasekaran[1], Dr. Bhavani M[2]
[1,2]*Solamalai College of Engineering*

Abstract - The increasing use of photovoltaics (PV) as a green energy resource has surged in recent years, primarily due to their integration with traditional power systems, which helps meet global energy needs and reduce carbon emissions. However, generating green electricity from this renewable source is often susceptible to power quality (PQ) disruptions caused by the intermittent nature of PV systems and other factors related to the electric grid, power converters, and connected loads. These disruptions must be minimized to prevent deterioration of the PQ in the studied system, which includes PV, DC-DC, and DC-AC converters, filters, the power grid, and control schemes. Without proper management of the DC-DC converter, deviations from the maximum power point (MPP) of the PV system will occur. To maximize the energy harvested from the PV system, this research developed MPP tracking (MPPT) algorithms using Modular Probabilistic Neural Network (MPNN) to adjusts the VDC reference signal of the inverter VDC regulator to achieve maximum power extraction from the PV array. Simulation results demonstrated that MPNN outperformed in tracking maximum power.

Key Words - Renewable source, Probabilistic Neural Network, Modular Probabilistic Neural Network, Maximum power point Tracking.

I INTRODUCTION

The use of renewable energy sources (RESs), particularly solar photovoltaic (PV), has increased and evolved globally as they provide a clean and secure alternative to fossil fuels, which are eventually going to be depleted. Initially, PV panels were primarily used in large factories and space missions before becoming more common in [1] explored the development of PV technologies, focusing on the materials used for cells and the environmental conditions affecting their efficiency. PV systems can function in both off-grid and on-grid modes. As a promising substitute for traditional non-renewable energy sources and a pollution-free option, grid-connected PV (GCPV) technology has garnered significant interest from both corporations and academia [2].

Photovoltaic (PV) systems are considered a key renewable energy source for future electricity generation. These systems convert photon energy into electrical energy. Due to their low voltage output, high step-up DC/DC converters are used in various applications, such as fuel cell technology, wind power, and solar systems, to increase the voltage [3] [4]. The rising demand for electricity, along with the high cost and limited availability of traditional energy sources, has made PV an attractive alternative. PV systems offer benefits such as availability, zero emissions, and low operation and maintenance costs, necessitating their increased use in both standalone and grid-connected configurations [5], [6] . Despite the challenges related to location, timing, seasonal variations, and atmospheric conditions, as well as the high implementation costs, running PV systems near their maximum power point (MPP) significantly improves their efficiency and helps achieve the maximum power output [7].

The power generated by grid-connected photovoltaic (GCPV) systems is affected by weather fluctuations, preventing them from operating at maximum capacity. To address this, researchers are exploring maximum power point tracking (MPPT) techniques to ensure PV systems operate at their peak efficiency despite weather variations[8],[9]. Various MPPT methods are employed with power electronic devices under consistent radiation. The most commonly used online techniques include perturb and observe (P&O), hill

climbing (HC), artificial neural networks (ANN), fuzzy logic, and incremental conductance (IN) [10]. Additionally, offline methods such as constant voltage, constant current, and curve fitting have been extensively described [11]. Hybrid algorithms have also been implemented to manage conditions like partial shading or non-uniform radiation [12] and [13]. One of the main challenges with photovoltaic (PV) power systems, especially at the point of common coupling (PCC), is maintaining power quality (PQ) [14]. Issues such as voltage and current harmonics arise due to variable solar irradiation, grid faults, and nonlinear loads involving advanced power electronics. Harmonic distortion (HD) negatively impacts the power grid by disrupting normal operations, causing overheating in connected devices, reducing the accuracy of electrical meters, interfering with communication lines, and increasing the current demand [15] . Studies have compared Brazilian standards for grid-connected PV (GCPV) inverters with those in Europe and the US, and analyzed voltage and current harmonics at the PCC of a GCPV system using the ICA method [16]. A harmonic management technique was proposed to keep the total harmonic distortion (THD) within acceptable limits after assessing the prevalence of current THD in the GCPV structure [17].

The primary power components of a typical grid-connected photovoltaic (GCPV) system are the inverter and the passive filter. In three-phase systems, particularly for high-power applications, multilevel inverters (MLIs) are preferred due to their low switching frequency. However, for small-scale household setups, a current-controlled two-level inverter is commonly used as a power conditioner. These systems can introduce undesirable harmonic currents into the grid, reducing overall efficiency. Consequently, standards such as IEEE-519 and IEEE-1547 have been established to limit the introduction of these harmonics [18]. To comply with these standards, a low-pass filter is necessary between the inverter and the grid at all power levels [19].

Designing the optimal passive filter for grid-connected systems is complex, as factors like potential resonance between the filter circuit and system impedance must be considered [20]. Achieving an optimal first-order L-filter that meets the requirements affordably is challenging with standard design methods. High-order passive filter topologies provide better harmonic attenuation with lower total inductance, thus reducing the filter's size and cost [21]. Power quality issues, including the production of voltage and current harmonic distortions (HDs), are primarily caused by fluctuations in solar irradiance and the use of advanced power electronic devices [22].

Harmonic distortions (HDs) in electrical systems have been addressed using various methods, including passive and active filters. For instance, an LCL filter with a shunt damping resistor was shown to reduce total harmonic distortion (THD) to 0.26%, outperforming L and LC structures in mitigating harmonics [23]. Another study demonstrated a hybrid damping approach using a parallel RC circuit and a digital filter [24]. In a different approach, a shunt active filter combined with the d-q regulating method reduced current THD from 27.3% to 3.9% in a developed GCPV system[25]. A hybrid damping strategy incorporating both passive and active damping techniques achieved a current THD of 3.7% [26].

Further research investigated the d-q shunt active filter and incremental conductance (INC) method for maximum power point (MPP) monitoring, which helped maintain current THD within acceptable limits. This study proposed using an artificial neural network (ANN) controller for DC bus voltage management instead of the traditional proportional-integral (PI) controller, resulting in a reduction of current THD to 3.2% [27]. Besides filters, other techniques for harmonic suppression have also been explored. For example, comparing a 127-level multi-level inverter (MLI) with lower-level MLIs showed that the 127-level MLI reduced current THD to 2.33% [28]. Additionally, the use of direct power control methodology improved the operation and energy efficiency of the pulse width modulation (PWM) inverter in a GCPV system, with positive results.

The energy efficiency and operation of a grid-connected photovoltaic (GCPV) system's pulse width modulation (PWM) inverter were enhanced using a direct power control methodology, which simulation results indicated had beneficial effects. Harmonic limits for system voltages ranging from 120 to 69 kV were detailed in previous studies [29]. This study aims to develop a GCPV system that meets these requirements and standards using advanced techniques. The system configuration includes a two-level converter, a boost converter, an LCL filter, and a

PV array. The management system's architecture is designed in the d-q reference frame [30]. Results from simulations and experimental implementations show that the proposed inverter, LCL filter, and maximum power point tracking (MPPT) algorithm effectively reduce harmonic voltage from 12.73% to 0.03% and harmonic current from 13.92% to 0.028%.

This study makes a significant contribution by applying two MPPT methods—artificial neural network (ANN) and cuckoo search (CS)—to grid-connected photovoltaic (GCPV) systems. These methods adjust the duty cycle (D) of the DC-DC converter to reflect changes in the maximum power point (MPP). The performance of the ANN and CS techniques is compared, revealing that the ANN method outperforms the CS algorithm in terms of performance and speed of dynamic responsiveness across several control indices, including overshoot, rise time, and transient response.

To maintain voltage and current total harmonic distortion (THD) at higher switching frequencies within prescribed limits, an effective LCL filter is designed using genetic algorithms (GA) and generalized reduced gradient (GRG) methods. The results demonstrate the superiority of the GRG method. By incorporating these advanced techniques, the point of common coupling (PCC) achieves appropriate levels of power quality (PQ), complying with updated standards. The simulation results show that implementing effective control and compliance mechanisms successfully mitigates PQ issues to the required standard levels.

The paper is organized as follows: Section II maximum power point tracking algorithms. Section III presents MPPT interfacing. Section IV deals with probabilistic neural networks Section V discusses the proposed modular probabilistic neural network. Section VI and VII provides the simulation setup, and result and discussion of the proposals. Finally, the conclusions are presented in the last section.

II MAXIMUM POWER POINT TRACKING ALGORITHMS

A typical solar panel converts only 30 to 40 percent of the incident solar energy into electrical power. To enhance the efficiency of solar panels, the Maximum Power Point Tracking (MPPT) technique is employed. This technique is based on the Maximum Power Transfer theorem, which states that power output is maximized when the Thevenin impedance of the circuit (source impedance) matches the load impedance. Therefore, the task of tracking the maximum power point is essentially an impedance matching problem.

On the source side, a boost converter is connected to the solar panel to increase the output voltage, making it suitable for various applications, such as driving a motor load. By appropriately adjusting the duty cycle of the boost converter, we can match the source impedance to the load impedance.

The Perturb & Observe algorithm works by making small adjustments to the operating voltage of the PV panel. If a small increase in voltage results in a positive change in power (ΔP), it indicates that the system is moving towards the Maximum Power Point (MPP), and further perturbations should continue in the same direction. Conversely, if the change in power (ΔP) is negative, it means the system is moving away from the MPP, and the direction of the perturbation should be reversed.

III MPPT INTERFACING

A controlled voltage source and a current source inverter are used to connect the modeled solar panel with the rest of the system and the boost converter, utilizing MATLAB's Sim Power Systems module. The block diagram in the figure demonstrates a simulation where a varying voltage output is observed. This model compares the power output when using an MPPT algorithm versus when not using one.

To facilitate this comparison, the model includes a manual switch. When the switch is set to the left, the circuit bypasses the MPPT algorithm, providing power, voltage, and current outputs through the respective scopes. When the switch is set to the right, the MPPT function block is included in the circuit, and the desired outputs are obtained through the respective scopes.

A boost converter is utilized in our simulation, applicable to real-world scenarios such as charging battery banks, running DC motors, and solar water pumping. The simulation is conducted with a 300Ω resistive load. Efficient motor operation requires load resistance matching techniques. In the boost converter circuit, an inductor of 0.763 mH and a capacitor of 0.611 μF are selected to ensure a ripple-free current.

The system includes a PI controller to regulate the input voltage of the boost converter. The MPPT algorithm calculates the reference voltage (Vref) towards which the PV operating voltage should move to maximize power output. This calculation is updated periodically at a rate of 1-10 samples per second. The PI controller acts as an external control loop, adjusting the input voltage by varying the duty cycle.

Pulse width modulation (PWM) is performed in the PWM block at a high switching frequency of 100 kHz. In our simulation, the proportional gain (KP) is set to 0.006 and the integral gain (KI) to 7. A higher KI value ensures faster system stabilization. The PI controller minimizes the error between Vref and the measured voltage by adjusting the duty cycle, which controls a MOSFET switch through its gate voltage.

IV PROBABILISTIC NEURAL NETWORKS

Among the most effective methodologies in artificial intelligence (AI) for modeling the behavior of artificial neural networks (ANNs) is the AI system itself, which serves as a paradigm for interpreting data. ANNs are composed of numerous basic units called neurons that work together concurrently to solve complex problems. This method iteratively adjusts the outputs to match the target until the network's output aligns with the objective, requiring a substantial number of input/target combinations for retraining.

An ANN typically consists of three layers: input, hidden, and output layers. The input layer receives and distributes inputs to the hidden layer's synapses, while the hidden layer performs intermediary computations to produce an accurate output in the output layer. The final architecture of the ANN is determined after conducting various experiments.

The Probabilistic Neural Network (PNN) applies Bayesian decision strategies to adjust Vdc, functioning as a supervised learning network. With sufficient training data, a PNN can converge to a Bayesian classifier. This type of network does not require traditional learning processes or initial weight settings, making it well-suited for real-time fault diagnosis and signal classification due to its fast learning and prediction capabilities.

In a PNN, input values are directly passed to the second layer, known as the pattern layer, without modification. Each training exemplar is represented by a unique pattern unit in this layer, with weight vectors mirroring the exemplar. During training, the appropriate weight vector is added to the network. For Vdc reference adjustment, are adjusted based on the probabilistic density function, which is the core principle of PNN. The process can be described by equation 1 and 2

$$f_k(X) = \frac{1}{N_k}\sum_{j=1}^{N_k} exp\left(\frac{\|X-X_{kj}\|}{2\sigma^2}\right) \qquad (1)$$

By modifying and applying the above equation (1) to the output vector H of the hidden layer in the hidden layer in the architecture.

$$H_h = exp\left(\frac{\sum_i (X-X_{kj})^2}{2\sigma^2}\right) \qquad (2)$$

$\text{Net}_j = \frac{1}{N_k}\sum_h N_{nj}^{hy} H_h$ and $\text{N}_j = \sum_h W_{nj}^{hy}$

$\text{Net}_j max_k(net_k)$ then $y_i = 1$, else $y_j = 0$

Where

i = number of input layers,h = number of hidden layers,j = number of output layers,k = number of training exemplars,N = number of classifications,σ = smoothing parameters, X= input vector and where $\|X - X_{kj}\|$ is the Euclidean distance between the vectors$X$ andX_{kj} i.e.,

$\|X - X_{kj}\| = \sum_i (X - X_{kj})^2, W_i^{xh}$ is the connection weight between the input layer X and M and W_{nj}^{hy} is the connection weight between the hidden layer and the output layers.

V MODULAR PROBABILISTIC NEURAL NETWORK

In a Modular Probabilistic Neural Network (MPNN), tasks are divided into several independent sub-tasks that operate in parallel. This architecture is straightforward, with components functioning independently of one another, contributing to a faster convergence rate due to task subdivision. Similar to a standard PNN, the MPNN comprises three layers: input, hidden, and output. The hidden layer calculates the distance between new, unknown inputs and training data. The number of input and hidden nodes depends on the predictor variables and exemplars, while the output nodes are determined by the predicted variables.

The modular structure is designed using Gaussian functions and kernel-based approximations to estimate the probability density function for classification problems. To avoid redundant training and efficiency,

the PNN employs an incremental learning process, which leverages its statistical characteristic to reduce training time and enhance classification accuracy

VI SIMULATION SETUP

The PV array comprises 86 parallel strings, with each string consisting of 7 SunPower SPR-415E modules connected in series. It's important to note that the model menu allows plotting of the I-V and P-V characteristics for either the selected module or the entire array shown in Figure 1.

The converter is implemented using a 3-level IGBT bridge PWM-controlled setup. To filter out harmonics generated by the IGBT bridge, an inverter choke RL and a small harmonics filter C are utilized. Connecting the inverter to the utility distribution system is a 250-kVA, 250V/25kV three-phase transformer.

The control system incorporates five main Simulink-based subsystem .Based on the 'Perturb and Observe' technique, this controller adjusts the VDC reference signal of the inverter VDC regulator to achieve maximum power extraction from the PV array.

VDC Regulator: Determines the active current (Id) reference required for the current regulator. Using Id and a zero-setting for Iq (reactive current), this regulator calculates the necessary reference voltages for the inverter. Essential for synchronization and accurate voltage/current measurements.

Generates firing signals to the IGBTs based on the required reference voltages, with a carrier frequency set to 1980 Hz (33*60).

The grid simulation replicates a typical North American distribution grid, featuring two 25-kV feeders, loads, grounding transformer, and an equivalent 120-kV transmission system.

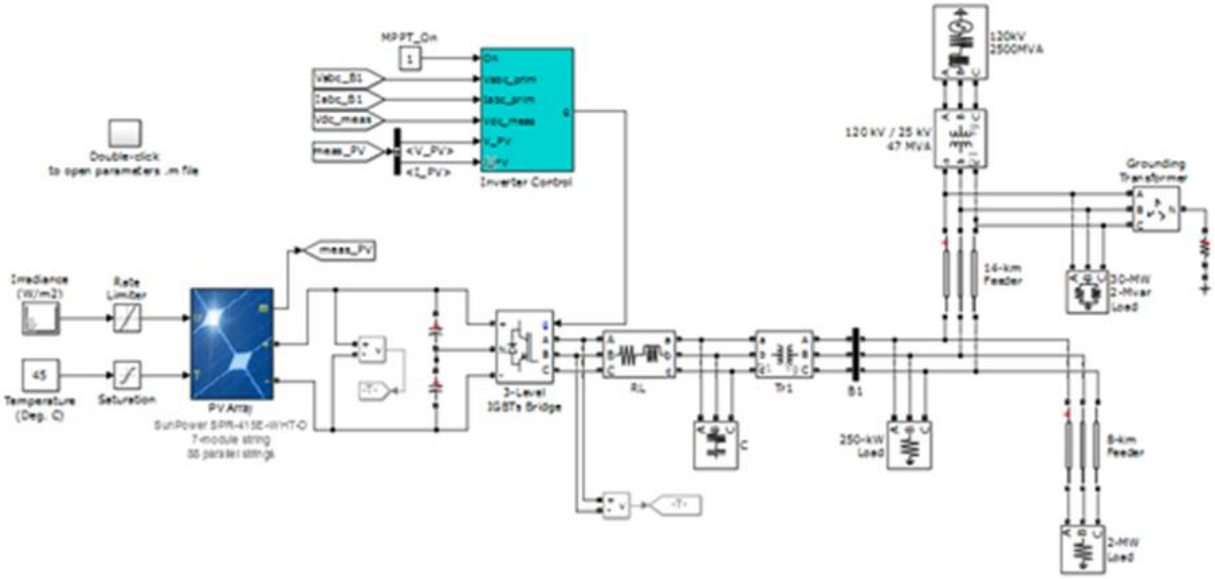

Fig.1 simulation setup

VII RESULT AND DISCUSSION

During simulation, initial irradiance input to the PV array model is 1000 W/m², with an operating temperature of 45°C. Steady-state conditions are achieved around t=0.15 seconds, resulting in a PV voltage (Vdc_mean) of 483 V and extracted power (Pdc_mean) from the array amounting to 240 kW. These values align closely with the specifications provided by the PV module manufacturer.

At t=0.3 seconds, the sun irradiance rapidly decreases from 1000 W/m² to 200 W/m². Through MPPT operation, the control system adjusts the VDC reference to 468 V, optimizing power extraction from the PV array to 48 kW without incorporating PNN shown in figure 13.

To improve the MPPT performance PNN and MPNN is used. The algorithm stands out from other techniques because it trains a network of networks instead of just one network. It begins by initializing all weights randomly and trains each network. The main

function of MPNN is to find the appropriate Vdc. In MPNN implementation 80% of the generated inputs used for training and 20% for testing. If a network achieves the minimum required error, its weights are recorded for testing; otherwise, the algorithm continues to refine the weights. After training, test signals evaluate the performance of the trained MPNN. Randomly selected signals from 100 power quality problems are used to test MPNN Figure 2 to figure 12 various key parameters related to MPPT is exhibited such as response of irradiance, DC mean, Pdc mean, V_PV, I_PV, I_diode plots between Vdc and Idc with their references Iq, Va and Vref_phase A.

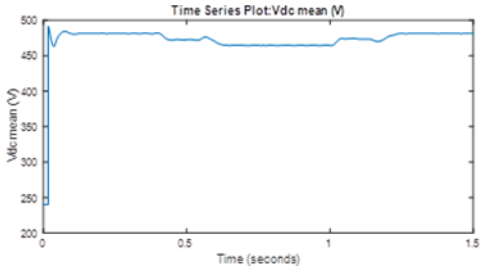

Fig.2 Irradiance

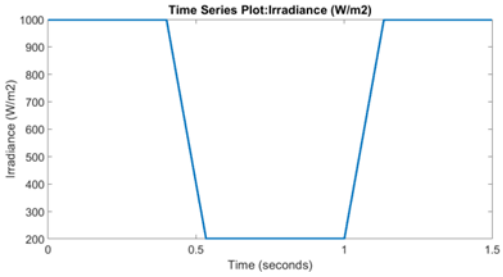

Fig.3 Plot of Vdc mean

Fig.4 Plot of Pdc mean

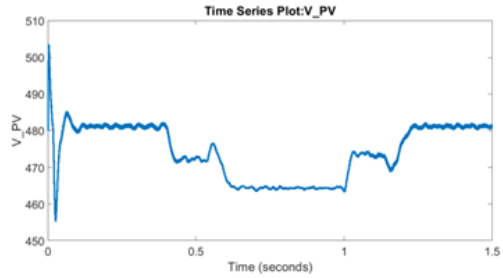

Fig.5 plot of V_PV

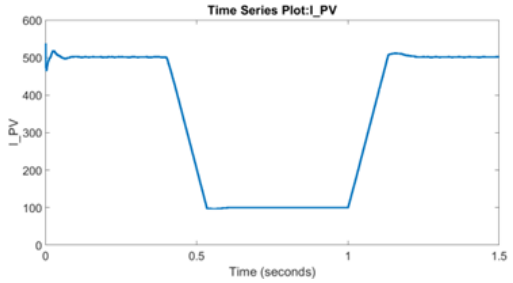

Fig.6 plot of I_PV

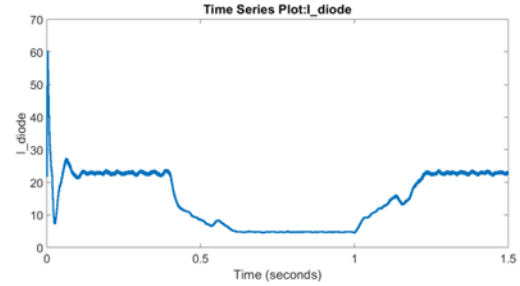

Fig.7 plot of I_diode

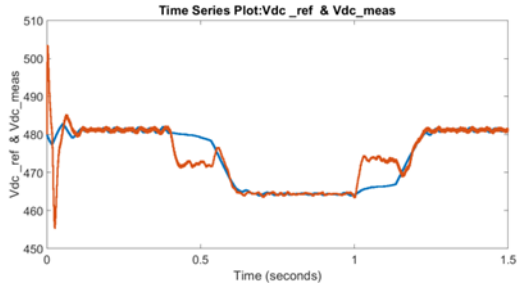

Fig.8 plot of Vdc

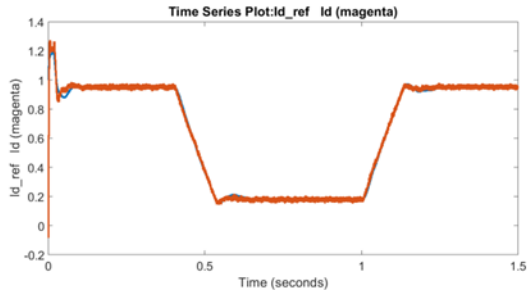

Fig.9 plot of Id

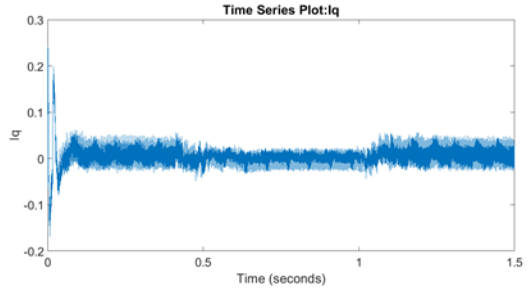

Fig.10 plot of Iq

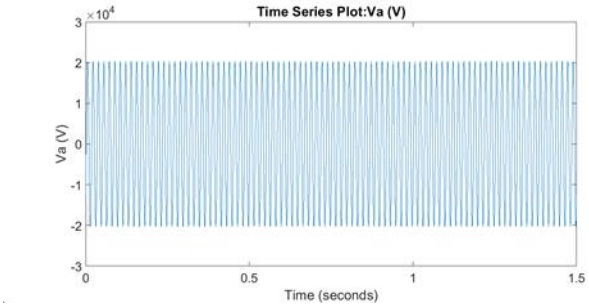

Fig.11 plot of Va

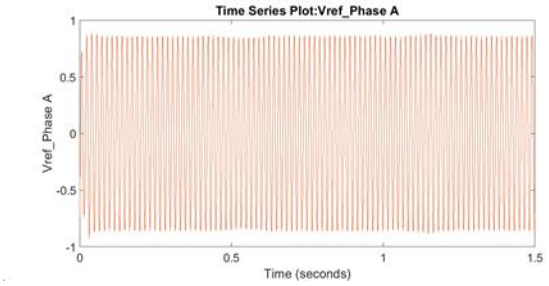

Fig.12 plot of Vref_Phase A

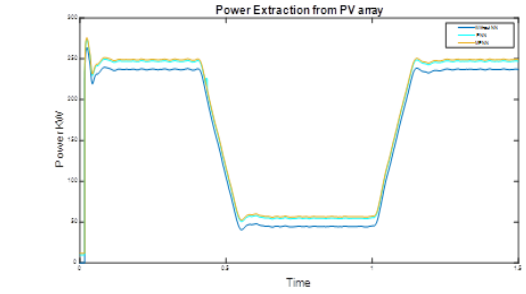

Fig.13 plot of power

VIII CONCLUSION

In this paper, the application of MPNN technique to adjusts the VDC reference signal of the inverter VDC regulator to achieve maximum power extraction from the PV array. As increasing use of photovoltaics has raised in recent years, primarily due to their integration with traditional power systems, which helps meet global energy needs. However, generating renewable source is often susceptible to power quality (PQ) issues caused by the intermittent nature of PV systems and other factors related to the electric grid, power converters, and connected loads. These disruptions must be minimized to prevent deterioration of the PQ and to maximize the energy harvested from the PV system, this paper developed MPP tracking (MPPT) algorithms using Modular Probabilistic Neural Network (MPNN) to adjusts the VDC reference signal. Simulation results demonstrated that MPNN outperformed in tracking maximum power.

REFERENCE

[1] H. K. Jahan, M. Abapour, K. Zare, S. H. Hosseini, F. Blaabjerg, and Y. Yang, ‘‘A multi level inverter with minimized components featuring self balancing and boosting capabilities for PV applications,’’ IEEE J. Emerg. Sel. Topics Power Electron., vol.11, no.1, pp. 1169–1178, Feb.2023, doi: 10.1109/JESTPE. 2019. 2922415.

[2] V. V. Tyagi, N. A. A. Rahim, N. A. Rahim, and J. A. L. Selvaraj, ‘‘Progress in solar PV technology: Research and achievement,’’ Renew. Sustain. Energy Rev., vol. 20, pp. 443–461, Apr. 2013, doi: 10.1016/j.rser.2012.09.028.

[3] K.Kumari and A.K.Jain, ‘‘Sensor reduction of a PV-gridtied system with tripartite control based on LCL filter,’’ IET Energy Syst. Integr., vol. 4, no. 3, pp. 409–419, Sep. 2022, doi: 10.1049/esi2.12072.

[4] M. M. Mahmoud, H. S. Salama, M. Bajaj, M. M. Aly, I. Vokony, S. S. H. Bukhari, D. E. M. Wapet, and A.-M.-M. Abdel-Rahim, ‘‘Integration of wind systems with SVC and STATCOM during various events to achieve FRT capability and voltage stability: Towards the reliability of modern power systems,’’ Int. J. Energy Res., vol. 2023, pp. 1–28, Feb. 2023, doi: 10.1155/2023/8738460.

[5] N. K. Saxena, A. R. Gupta, S. Mekhilef, W. D. Gao, A. Kumar, V. Gupta, R. S. Netto, and A. Kanungo, ‘‘Firefly algorithm based LCL filtered grid-tied STATCOM design for reactive power compensation in SCIG based micro-grid,’’ Energy Rep., vol. 8, pp. 723–740, Nov. 2022, doi: 10.1016/j.egyr.2022.07.106.

[6] H. Boudjemai, S. A. E. M. Ardjoun, H. Chafouk, M. Denai, Z. M. S. Elbarbary, A. I. Omar, and M. M. Mahmoud, ‘‘Application of a novel synergetic control for optimal power extraction of a small-scale wind generation system with variable loads and wind speeds,’’ Symmetry, vol. 15, no. 2, p. 369, Jan. 2023, doi: 10.3390/sym15020369.

[7] V. R. Chowdhury and A. Singh, ‘‘Adaptive internal model based current control with embedded active damping of a three-phase grid connected inverter with LCL filter for PV

application,'' in Proc. IEEE Energy Convers. Congr. Expo. (ECCE), Oct. 2022, pp. 1–6, doi: 10.1109/ECCE50734.2022.9947896.

[8] S. Foteinis, N. Savvakis, and T. Tsoutsos, ''Energy and environmental performance of photovoltaic cooling using phase change materials under the Mediterranean climate,'' Energy, vol.265, Feb.2023,Art. no. 126355, doi: 10.1016/j.energy.2022.126355.

[9] G.Walker, ''Evaluating MPPT converter topologies using a MATLABPV model,'' J. Electr. Electron. Eng. Aust., vol. 21, no. 1, pp. 49–55, 2001.

[10] A. S. Chatterjee, ''A bus clamping PWM-based improved control of grid tied PV inverter with LCL filter under varying grid frequency condition,'' IETE J. Res., vol. 69, no. 2, pp. 862–878, Feb. 2023, doi: 10.1080/ 03772063.2020.1844067.

[11] V.R.Vakacharla, K.Gnana, P.Xuewei, B.L.Narasimaharaju, M.Bhukya, A. Banerjee, R. Sharma, and A. K. Rathore, ''State-of-the-art power electronics systems for solar-to-grid integration,'' Sol. Energy, vol. 210, pp. 128–148, Nov. 2020, doi: 10.1016/j.solener.2020.06.105.

[12] B. Yang, T. Zhu, J. Wang, H. Shu, T. Yu, X. Zhang, W. Yao, and L. Sun, ''Comprehensive overview of maximum power point tracking algorithms of PV systems under partial shading condition,'' J.CleanerProd., vol.268, Sep. 2020, Art. no. 121983, doi: 10.1016/j.jclepro. 2020.121983.

[13] [M. Hosseinpour and N. Rasekh, ''A single-phase grid-tied PV based Trans-Z-source inverter utilizing LCL filter and grid side current active damping,'' J. Energy Manag. Technol., vol. 3, no. 3, pp. 67–77, 2019.

[14] E. Rakhshani, K. Rouzbehi, A. J. Sánchez, A. C. Tobar, and E. Pouresmaeil, ''Integration of large scale PV-based generation into power systems: A survey,'' Energies, vol. 12, no. 8, p. 1425, Apr. 2019, doi: 10.3390/en12081425.

[15] D. P. Mishra, K. K. Rout, S. Mishra, M. Nivas, R. K. P. R. Naidu, and S. R. Salkuti,''Power quality enhancement of grid-connected PV system,'' Int. J. Power Electron. Drive Syst., vol. 14, no. 1, pp. 369–377, 2023, doi: 10.11591/ ijpeds. v14.i1. pp369-377.

[16] P. S. de Oliveira, M. A. A. Lima, A. S. Cerqueira, C. A. Duque, and D. D. Ferreira, ''Harmonic analysis based on scica at PCC of a grid-connected micro solar PV power plant,'' in Proc. 18th Int. Conf. Harmon. Quality Power (ICHQP), May 2018, pp. 1–6, doi: 10.1109/ICHQP. 2018.8378875.

[17] A. Vinayagam, A. Aziz, P. M. Balasubramaniyam, J. Chandran, V. Veerasamy, and A.Gargoom, ''Harmonics assessment and mitigationin a photovoltaic integrated network,'' Sustain. Energy, Grids Netw., vol. 20, Dec. 2019, Art. no. 100264, doi: 10.1016/ j.segan. 2019.100264.

[18] S. K. Das, M. K. Sinha, and A. K. Prasad, ''Designing and simulation of double stage grid-linked PV system using MATLAB/simulink,'' in Recent Advances in Power Systems (Lecture Notes in Electrical Engineering), vol. 960, 2023, pp. 169–195, doi: 10.1007/978-981-19-6605-7_13.

[19] R. Chen, J. Zeng, X. Huang, and J. Liu, ''An H∞ filter based active damping control strategy for grid-connected inverters with LCL filter applied to wind power system,'' Int.J.Electr. Power EnergySyst., vol.144, Jan. 2023, Art. no. 108590, doi: 10.1016/j.ijepes.2022.108590.

[20] B. Supriya, K. Palle, A. Bhanuchandar, R. Sakile, D. Vamshy, and K. B. Kumar, ''A current control scheme of three phase three-level neutral point clamped grid connected inverter using min–max algorithm approach,'' in Smart Energy and Advancement in Power Technologies (Lecture Notes in Electrical Engineering), vol. 927, 2023, pp. 257–266, doi: 10.1007/978-981-19-4975-3_20.

[21] A. Tripathi, S. P. Soundharya, R. Vigneshwar, and M. R. Rashmi, ''Concatenation of SEPIC and matrix converter with LCL filter for vehicle to grid application,'' in Pervasive Computing and Social Networking (Lecture Notes in Networks and Systems), vol. 475, 2023, pp. 743–757, doi: 10.1007/978-981-19-2840-6_56.

[22] D.Datta,S.K.Sarker, and M.R.I.Sheikh, ''Design ing a unified damping and cross-coupling rejection controller for LCL filtered PV-based islanded microgrids,'' Eng. Sci. Technol., Int.J., vol.35, Nov.2022, Art. no. 101244, doi: 10.1016/j.jestch.2022.101244.

[23] R. Xu, L. Xia, J. Zhang, and J. Ding, ‘‘Design and research on the LCL filter in three-phase PV grid-connected inverters,’’ Int. J. Comput. Electr. Eng., vol. 5, no. 3, pp. 322–325, 2013, doi: 10.7763/ijcee.2013.v5.723.

[24] S. Adak, H. Cangi, and A. S. Yilmaz, ‘‘Design of an LLCL type filter for stand-alone PV systems’ harmonics,’’ J. Energy Syst., vol. 3, no. 1, pp. 36–50, Mar. 2019, doi: 10.30521/jes.506076.

[25] Y. Lei, W. Xu, C. Mu, Z. Zhao, H. Li, and Z. Li, ‘‘New hybrid damping strategy for grid-connected photovoltaic inverter with LCL filter,’’ IEEE Trans. Appl. Supercond., vol. 24, no. 5, pp. 1–8, Oct. 2014, doi: 10.1109/ TASC. 2014.2351237.

[26] H. Yu, J. Pan, and A. Xiang, ‘‘A multi-function grid-connected PV system with reactive power compensation for the grid,’’Sol. Energy, vol.79, no.1, pp. 101–106, Jul. 2005, doi: 10.1016/j.solener.2004.09.023.

[27] M. Andela, A. Shaik, S. Beemagoni, V. Kurimilla, R. Veramalla, A. Kodakkal, and S.R.Salkuti,‘‘Solar photovoltaic system-based reduced switch multilevel inverter for improved power quality,’’ Clean Technol., vol. 4, no. 1, pp. 1–13, Jan. 2022, doi: 10.3390/ clean technol 4010001.

[28] A. Fekik, M. L. Hamida, H. Houassine, A. T. Azar, N. A. Kamal, H. Denoun, S. Vaidyanathan, and A. Sambas, ‘‘Power quality improvement for grid-connected photovoltaic panels using direct power control,’’ in Modeling and Control of Static Converters for Hybrid Storage Systems, 2021, pp. 107–142, doi: 10.4018/978-1-7998-7447-8. ch005.

[29] D. Prasad, N. Kumar, and R. Sharma, ‘‘Shunt active power filter based on synchronous reference frame theory connected to SPV for power quality enrichment,’’ in Machine Learning, Advances in Computing, Renewable Energy and Communication (Lecture Notes in Electrical Engineering), vol. 768, 2022, pp. 281–292, doi: 10.1007/978-981-16-2354-7_26.

[30] W. A. A. Salem, W. G. Ibrahim, A. M. Abdelsadek, and A. A. Nafeh, ‘‘Grid connected photovoltaic system impression on power quality of low voltage distribution system,’’ Cogent Eng., vol. 9, no. 1, Dec. 2022, Art. no. 2044576, doi: 10.1080/23311916.2022.2044576.